Structure-Preserving Model Reduction for Dissipative Mechanical Systems

Rebekka S. Beddig, Peter Benner, Ines Dorschky, Timo Reis, Paul Schwerdtner, Matthias Voigt, and Steffen W. R. Werner

Abstract Suppressing vibrations in mechanical models, usually described by second-order dynamical systems, is a challenging task in mechanical engineering in terms of computational resources even nowadays. One remedy is structure-preserving model order reduction to construct easy-to-evaluate surrogates for the original dynamical system having the same structure. In our work, we present an overview of our recently developed structure-preserving model reduction methods

——————————

Rebekka S. Beddig
Hamburg University of Technology, Institute of Mathematics, Am Schwarzenberg-Campus 3, Gebäude E, 21073 Hamburg, Germany, e-mail: rebekka.beddig@tuhh.de

Peter Benner
Max Planck Institute for Dynamics of Complex Technical Systems, Sandtorstraße 1, 39106 Magdeburg, Germany, e-mail: benner@mpi-magdeburg.mpg.de
Otto von Guericke University Magdeburg, Faculty of Mathematics, Universitätsplatz 2, 39106 Magdeburg, Germany, e-mail: peter.benner@ovgu.de

Ines Dorschky
Universität Hamburg, Department of Mathematics, Center for Optimization and Approximation, Bundesstraße 55, 20146 Hamburg, Germany, e-mail: ines.dorschky@uni-hamburg.de

Timo Reis
Universität Hamburg, Department of Mathematics, Center for Optimization and Approximation, Bundesstraße 55, 20146 Hamburg, Germany, e-mail: timo.reis@uni-hamburg.de

Paul Schwerdtner
Technische Universität Berlin, Institut für Mathematik, Straße des 17. Juni 136, 10623 Berlin, Germany, e-mail: schwerdt@math.tu-berlin.de

Matthias Voigt
Universität Hamburg, Department of Mathematics, Center for Optimization and Approximation, Bundesstraße 55, 20146 Hamburg, Germany, e-mail: matthias.voigt@uni-hamburg.de
Technische Universität Berlin, Institut für Mathematik, Straße des 17. Juni 136, 10623 Berlin, Germany, e-mail: mvoigt@math.tu-berlin.de

Steffen W. R. Werner
Max Planck Institute for Dynamics of Complex Technical Systems, Sandtorstraße 1, 39106 Magdeburg, Germany, e-mail: werner@mpi-magdeburg.mpg.de

for second-order systems. These methods are based on modal and balanced truncation in different variants, as well as on rational interpolation. Numerical examples are used to illustrate the effectiveness of all described methods.

1 Introduction

We consider model order reduction of dynamical systems arising from modeling of mechanical systems, which have the property of *dissipativity*. That is, energy is only consumed and not produced by the system. In the particular focus of this work are *linear second-order systems*

$$M\ddot{q}(t) + D\dot{q}(t) + Kq(t) = B_{\mathrm{u}}u(t),$$
$$y(t) = C_{\mathrm{p}}q(t) + C_{\mathrm{v}}\dot{q}(t) \tag{1}$$

with $M, D, K \in \mathbb{R}^{n \times n}$, $B_{\mathrm{u}} \in \mathbb{R}^{n \times m}$, and $C_{\mathrm{p}}, C_{\mathrm{v}} \in \mathbb{R}^{p \times n}$. These occur naturally by modeling mechanical systems via force balances, in which the second derivative of the position vector $q(t)$ at time $t \in \mathbb{R}$ occurs by Newton's second law. Hereby, the matrices M, D, and K are respectively called *mass matrix*, *damping matrix*, and *stiffness matrix*. The function $t \mapsto u(t)$ expresses the *input* to the system (external forces), a function that can be chosen by the operator (or, alternatively called, the "user") of the system. Moreover, the model contains an *output* $t \mapsto y(t)$, which contains some linear combinations of the state variables and its first derivative which are of particular interest. The typical situation is, especially for systems of high complexity, that the position vector $q(t)$ evolves in a high-dimensional space, that is, the number n is large. In contrast to that, the input and output spaces are low-dimensional, i.e., $m \ll n$ and $p \ll n$. Since the number n of position variables is a significant measure for the difficulty of the numerical simulation of (1), there is a need for efficient and reliable methods for model reduction, i.e., the approximation of such systems by ones whose solutions can be computed with significantly less effort. In this context, "reliable" means that the output of the reduced system is (mathematically proven to be) close to the output of the original system for the same input signal, whereas "efficient" means that the determination of the reduced system comes with as little effort as possible. Another important demand on model order reduction methods is that they preserve inherent properties such as stability and the second-order structure of the system (to mention only a few). By the latter, we mean that the reduced-order model is of the form

$$\widehat{M}\ddot{\widehat{q}}(t) + \widehat{D}\dot{\widehat{q}}(t) + \widehat{K}\widehat{q}(t) = \widehat{B}_{\mathrm{u}}u(t),$$
$$\widehat{y}(t) = \widehat{C}_{\mathrm{p}}\widehat{q}(t) + \widehat{C}_{\mathrm{v}}\dot{\widehat{q}}(t) \tag{2}$$

with $\widehat{M}, \widehat{D}, \widehat{K} \in \mathbb{R}^{r \times r}$, $\widehat{B}_{\mathrm{u}} \in \mathbb{R}^{r \times m}$, and $\widehat{C}_{\mathrm{p}}, \widehat{C}_{\mathrm{v}} \in \mathbb{R}^{p \times r}$ and with $r \ll n$. Moreover, models of mechanical systems have the property that the mass and stiffness matrices are positive definite, whereas the negative of the damping matrix is *dissipative*, that

is, $D + D^\top$ is positive semi-definite. These properties are requested to be preserved as well by the reduced system (2).

Meanwhile, model reduction is an established discipline within applied mathematics and is subject of textbooks and collections, see [1–5]. In particular, for first-order systems

$$
\begin{aligned}
\dot{x}(t) &= \mathscr{A}x(t) + \mathscr{B}u(t), \\
y(t) &= \mathscr{C}x(t),
\end{aligned}
\tag{3}
$$

there exists a rich theory for their approximation by reduced systems of low state-space dimension, see [1] for an overview. These methods are indeed applicable to first-order representations of second-order systems like

$$
\begin{bmatrix} I_n & 0 \\ 0 & M \end{bmatrix} \frac{\mathrm{d}}{\mathrm{d}t} \begin{bmatrix} q(t) \\ \dot{q}(t) \end{bmatrix} = \begin{bmatrix} 0 & I_n \\ -K & -D \end{bmatrix} \begin{bmatrix} q(t) \\ \dot{q}(t) \end{bmatrix} + \begin{bmatrix} 0 \\ B_\mathrm{u} \end{bmatrix} u(t),
$$

$$
y(t) = \begin{bmatrix} C_\mathrm{p} & C_\mathrm{v} \end{bmatrix} \begin{bmatrix} q(t) \\ \dot{q}(t) \end{bmatrix}.
$$

However, the problem with this is that the reduced system is again of first order, and it does in general not have a physical interpretation as a mechanical system. The structure-preserving model order reduction problem of second-order systems is therefore a problem on its own and new techniques have to be developed.

The model order reduction problem for linear time-invariant systems allows us to also consider the problem in the frequency domain. More precisely, the *transfer function* can be considered, which for (1) is given by

$$
H(s) = (C_\mathrm{p} + sC_\mathrm{v})(s^2 M + sD + K)^{-1} B_\mathrm{u} = \begin{bmatrix} C_\mathrm{p} & C_\mathrm{v} \end{bmatrix} \begin{bmatrix} sI_n & -I_n \\ K & sM + D \end{bmatrix} \begin{bmatrix} 0 \\ B_\mathrm{u} \end{bmatrix}.
$$

Plancherel's theorem [1, Prop. 5.1] gives a link between the time and frequency domain in a way that — very roughly speaking — "the better the transfer function of the reduced system approximates that of the original system, the better the outputs of original and reduced systems coincide". Two important measures for the distance between transfer functions are the $\mathscr{H}_\infty$-*norm*, which for stable systems expresses the supremal distance between the transfer functions on the imaginary axis; and the so-called *gap metric* [6], which applies to arbitrary, possibly unstable, systems and can be expressed by the $\mathscr{H}_\infty$-norm of certain stable factorizations of transfer functions. Whereas in the time domain the $\mathscr{H}_\infty$-norm expresses the L^2-norm differences of the outputs of the original and reduced system, the gap metric can be seen as a quantitative measure for the distance of the dynamics of systems.

Besides considering arbitrary linear outputs $y(t) = C_\mathrm{p}q(t) + C_\mathrm{v}\dot{q}(t)$, in our considerations special emphasis is put on *co-located* velocity outputs $y(t) = B_\mathrm{u}^\mathsf{T}\dot{q}(t)$, which corresponds to measurement of velocities directly at the force actuators forming the input. This special input-output configuration has the additional property that it provides an energy balance, namely

$$\forall t \geq 0: \qquad \frac{1}{2}\left(\dot{q}(t)^{\mathsf{T}}M\dot{q}(t) + q(t)^{\mathsf{T}}Kq(t)\right) - \frac{1}{2}\left(\dot{q}(0)^{\mathsf{T}}M\dot{q}(0) + q(0)^{\mathsf{T}}Kq(0)\right)$$

$$= \int\limits_0^t y(\tau)^{\mathsf{T}}u(\tau)\,\mathrm{d}\,\tau - \int\limits_0^t \dot{q}(\tau)^{\mathsf{T}}D\dot{q}(\tau)\,\mathrm{d}\,\tau.$$

The expressions $\frac{1}{2}\dot{q}(t)^{\mathsf{T}}M\dot{q}(t)$, $\frac{1}{2}q(t)^{\mathsf{T}}Kq(t)$, respectively, stand for the kinetic and potential energies of the system at time t, whereas $\int_0^t \dot{q}(\tau)^{\mathsf{T}}D\dot{q}(\tau)\,\mathrm{d}\,\tau$ is the dissipated energy, and $\int_0^t y(t)^{\mathsf{T}}u(t)\,\mathrm{d}t$ is the energy put into the system at the actuators within the time interval $[0,t]$. In particular, since $-D$ is dissipative and the mass and stiffness matrices are positive definite, in the case where the system is in a standstill at $t = 0$, i.e., $\dot{q}(0) = q(0) = 0$, this energy balance reduces to

$$\forall t \geq 0: \qquad 0 \leq \int\limits_0^t y(\tau)^{\mathsf{T}}u(\tau)\,\mathrm{d}\,\tau.$$

Systems with this property are called *passive*, a property which is further desired to be preserved by the reduced-order model. Note that the frequency domain pendant of passivity is *positive realness*, i.e., the transfer function $H(s)$ has no poles and is dissipative in the open right complex half plane.

For linear time-invariant systems, there are three "prominent" techniques for model order reduction, namely *modal-based*, *balancing-based*, and *interpolation-based* approaches. The modal-based methods consider eigenvalue problems associated with the potential poles of the transfer function to retain chosen poles from the original in the reduced-order model. Balancing-based methods use energy considerations to figure out parts of the state only contributing marginally to the input-output behavior, which are truncated to obtain a reduced system of a priori known quality by providing an error bound in the $\mathscr{H}_\infty$-norm or gap metric. The main cost in the determination of reduced-order models by balanced truncation is the numerical solution of matrix equations of Lyapunov or Riccati type. Interpolation-based methods use certain projections of the state-space which guarantee exactness of the transfer function of the reduced-order system at some prescribed frequencies.

For second-order systems, the general ideas of balancing-based model order reduction are subject of various contributions [7–14] (see also [15] for an overview). Some progress has been made in preservation of certain physical properties like passivity in model reduction of second-order systems with co-located inputs and outputs [13–15], but none of these methods are provided with an error bound. Besides these, there exist interpolatory methods, which succeed either in preserving the second-order structure [16, 17] or deliver a posteriori $\mathscr{H}_\infty$ error bounds [18]. However, all the approaches mentioned lack a combination of the two.

In the project "Structure-Preserving Model Reduction for Dissipative Mechanical Systems" of the DFG Priority Program "Calm, Smooth, and Smart - Novel Approaches for Influencing Vibrations by Means of Deliberately Introduced Dissipation" (SPP1897), three approaches for model order reduction of second-order systems have been developed. An extract of this work can be found in [19].

The structure of this report is as follows. In Section 2, we present our results on a dominant pole algorithm for modally damped mechanical systems. The reduction is hereby based on $q(t) \approx V\widehat{q}(t)$, where $V \in \mathbb{R}^{n \times r}$ contains eigenvectors of the matrix binomial $\lambda^2 M + \lambda D + K$, which are dominant in the sense that the corresponding residue contributes much to the transfer function. In Section 3, a novel balancing-based approach for second-order systems is presented. Hereby, so-called *frequency- and time-limited Gramians* are used to identify the dominant behavior of the system on some prescribed time and frequency intervals. In Section 4, we consider an alternative balancing-based method for second-order systems with co-located inputs and outputs. The method of *positive real balanced truncation* is considered for this class, and it is shown that this method yields a passive first-order reduced system with a special structure. It is proven that an error bound in the gap metric holds and, under some additional assumptions, a special state-space transformation leads to a second-order system realization. Section 5 is devoted to an interpolation-based model order reduction method for second-order systems. This method is established on an optimization-based technique, which generates a sequence of reduced-order models of descending error in the $\mathscr{H}_\infty$-norm.

2 A dominant pole algorithm for modally damped mechanical systems

One of the oldest model order reduction approaches, which also directly translates into a structure-preserving setting for second-order systems (1), is the *modal truncation method* [20]. Thereby, the projection basis for the reduced-order model only consists of the left and right eigenvectors corresponding to the desired eigenvalues. In case of second-order systems like (1), the corresponding quadratic eigenvalue problem

$$\left(\lambda_i^2 M + \lambda_i D + K\right) x_i = 0, \quad y_i^{\mathsf{H}} \left(\lambda_i^2 M + \lambda_i D + K\right) = 0 \tag{4}$$

has to be considered for the left and right eigenvectors $y_i, x_i \in \mathbb{C}^n \setminus \{0\}$ corresponding to the eigenvalue $\lambda_i \in \mathbb{C}$. Hereby, y^{H} stands for the conjugate transpose of y.

For this model order reduction method, the choice of the eigenvalues that remain in the reduced system is critical. Classical choices are, e. g., taking the rightmost eigenvalues in the complex plane or the eigenvalues with smallest absolute values. A significant drawback of those simple choices is the neglection of the input and output matrices, which have a significant influence on the actual input-to-output behavior of the system. The extension of the classical modal truncation method to a more sophisticated choice of eigenvalues is the *dominant pole algorithm* [21]. Here, the eigenvalues with the strongest influence on the system behavior are computed and then chosen for constructing the reduced-order model. Adaptations of the dominant pole algorithm to the case of general second-order systems have been

suggested in [22] for single-input single-output systems and in [23] for multi-input multi-output systems.

A modeling approach used very often for mechanical structures results in modally damped second-order systems. Hereby, for the second-order system (1) it is assumed that $C_v = 0$, M, D, K are symmetric positive definite and additionally it holds that $DM^{-1}K = KM^{-1}D$, i.e., the system can be rewritten into modal coordinates and completely decouples into independent mechanical systems of order 1; see, e.g., [24]. Classical damping approaches, like Rayleigh and critical damping, fall into this category. For this type of mechanical systems, the idea of the dominant pole algorithm can be reformulated. As shown in [24], choosing X as a scaled eigenvector basis gives

$$X^\mathsf{T}MX = \Omega^{-1} \quad \text{and} \quad X^\mathsf{T}KX = \Omega \tag{5}$$

with $\Omega = \mathrm{diag}(\omega_1, \ldots, \omega_n) \in \mathbb{R}^{n \times n}$ and $X = [x_1, \ldots, x_n] \in \mathbb{R}^{n \times n}$. By the modal damping assumption, we further get

$$X^\mathsf{T}DX = 2\Xi \tag{6}$$

with $\Xi = \mathrm{diag}(\xi_1, \ldots, \xi_n) \in \mathbb{R}^{n \times n}$. Combining (5) and (6), the transfer function of (1) can be written in pole-residue form

$$\begin{aligned}
H(s) &= C_\mathrm{p}(s^2 M + sD + K)^{-1}B_\mathrm{u} \\
&= C_\mathrm{p}X(s^2\Omega^{-1} + 2s\Xi + \Omega)^{-1}X^\mathsf{T}B_\mathrm{u} \\
&= \sum_{k=1}^{n} \frac{\omega_k C_\mathrm{p}x_k x_k^\mathsf{T} B_\mathrm{u}}{(s - \lambda_k^+)(s - \lambda_k^-)},
\end{aligned} \tag{7}$$

where the eigenvalue pairs λ_k^+, λ_k^- are given by

$$\lambda_k^\pm = -\omega_k \xi_k \pm \omega_k \sqrt{\xi_k^2 - 1}. \tag{8}$$

This new pole-residue formulation (7) is now used to derive a new dominant pole algorithm for modally damped second-order systems. With (7), the extension of a classical dominant pole as in [23] to pole pairs reads as: The pole pair $(\lambda_k^+, \lambda_k^-)$ is called dominant if it satisfies

$$\frac{\|\omega_k C_\mathrm{p}x_k x_k^\mathsf{T} B_\mathrm{u}\|_2}{Re(\lambda_k^+)Re(\lambda_k^-)} > \frac{\|\omega_j C_\mathrm{p}x_j x_j^\mathsf{T} B_\mathrm{u}\|_2}{Re(\lambda_j^+)Re(\lambda_j^-)} \quad \text{for all } j \neq k. \tag{9}$$

The corresponding dominant pole algorithm then computes the r most dominant pole pairs and the corresponding eigenvectors, such that the reduced-order model's transfer function is given by

(a) Sigma plots.

(b) Relative error.

——— Original model   - - - Reduced-order model ($r = 10$)
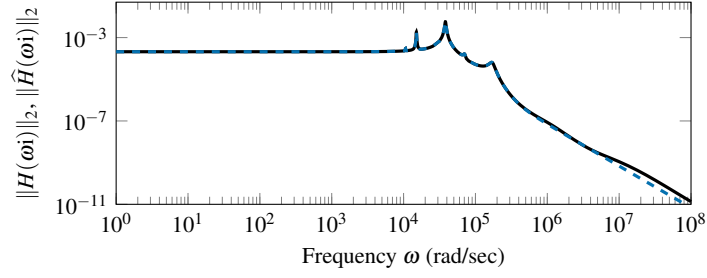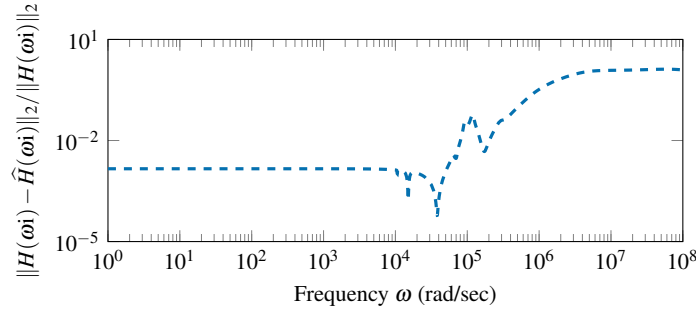
Fig. 1: Modally-damped dominant pole algorithm results for the butterfly gyroscope example.

$$\widehat{H}(s) = \sum_{k=1}^{r} \frac{\omega_k C_{\mathrm{p}} x_k x_k^{\mathsf{T}} B_{\mathrm{u}}}{(s - \lambda_k^+)(s - \lambda_k^-)} \approx H(s).$$

The projection basis is then given by the r eigenvectors corresponding to the chosen pole pairs. The resulting algorithm is published in [25]. Additionally, we published an implementation of this new algorithm for large-scale sparse systems as MATLAB toolbox [26].

Remark 1. A big advantage of this new approach, compared to the methods in [22] and [23], is the restriction to one-sided projections. This preserves the system and eigenvalue structure in each single step such that the resulting eigenvector basis will be real and no additional unrelated Ritz values, which usually disturb the resulting approximation, are introduced in the reduced-order model.

As an illustrative example, we consider the butterfly gyroscope benchmark from [27] with $n = 17\,361$, $m = 1$ and $p = 12$. The used Rayleigh damping for the $D\ (= 10^{-6} \cdot K)$ matrix belongs to the class of modal damping. We are using the implementation from [26] to compute a reduced-order model with the first 10 dominant
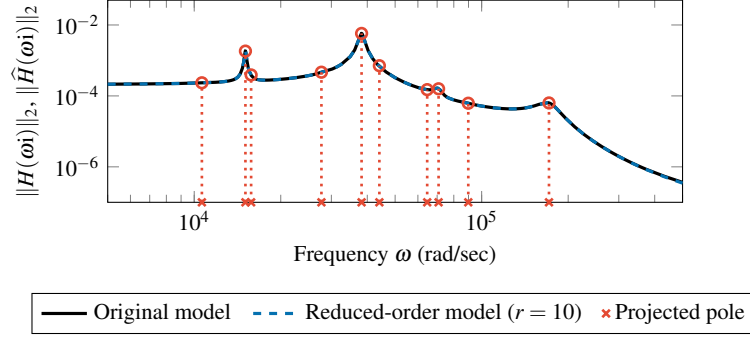
Fig. 2: Projection of the computed dominant poles on the frequency axis compared with the transfer functions for the butterfly gyroscope example.

pole pairs by the criterion (9). By construction, the resulting reduced-order model has order 10. Fig. 1 shows the results in the frequency domain with the frequency response behavior of the original and the reduced-order model and the point-wise relative error of the approximation. Up to a frequency of about 10^6 rad/sec, the behavior of the original system is well reproduced, while later, the two lines begin to slightly diverge. Additionally, Fig. 2 shows the position of the computed dominant poles as projection onto the imaginary axis and the corresponding transfer function behavior.

3 Second-order frequency- and time-limited balanced truncation

In practice, a global approximation of the system's behavior in either the frequency or time domain is often not required. The second-order limited balanced truncation approaches are a suitable tool for model order reduction restricted to certain frequency and time ranges. Thereby, the ideas from the first-order frequency- and time-limited balanced truncation methods [28] are combined with different second-order balanced truncation approaches [7, 11, 15]. A first version of the methods can be found in [19, 25, 29, 30] and the completed theory with applications to large-scale sparse systems is contained in [31].

The idea of the method is based on the first companion form realization of (1), which is given by

$$\underbrace{\begin{bmatrix} I_n & 0 \\ 0 & M \end{bmatrix}}_{=:\mathscr{E}} \dot{x}(t) = \underbrace{\begin{bmatrix} 0 & I_n \\ -K & -D \end{bmatrix}}_{=:\mathscr{A}} x(t) + \underbrace{\begin{bmatrix} 0 \\ B_\mathrm{u} \end{bmatrix}}_{=:\mathscr{B}} u(t),$$
$$y(t) = \underbrace{\begin{bmatrix} C_\mathrm{p} & C_\mathrm{v} \end{bmatrix}}_{=:\mathscr{C}} x(t). \tag{10}$$

For (10), the classical controllability and observability Gramians are defined and can be limited as in [28]. Therefore, the frequency-limited Gramians P_Ω and Q_Ω of (10) are the unique positive semi-definite solutions of the potentially indefinite Lyapunov equations

$$\mathscr{A} P_\Omega \mathscr{E}^\mathsf{T} + \mathscr{E} P_\Omega \mathscr{A}^\mathsf{T} + \mathscr{B}_\Omega \mathscr{B}^\mathsf{T} + \mathscr{B} \mathscr{B}_\Omega^\mathsf{T} = 0,$$
$$\mathscr{A}^\mathsf{T} Q_\Omega \mathscr{E} + \mathscr{E}^\mathsf{T} Q_\Omega \mathscr{A} + \mathscr{C}_\Omega^\mathsf{T} \mathscr{C} + \mathscr{C}^\mathsf{T} \mathscr{C}_\Omega = 0$$

for a specified frequency range $\Omega = [\omega_1, \omega_2] \cup [-\omega_2, -\omega_1]$. The right-hand side matrices contain matrix functions, which are given by

$$\mathscr{B}_\Omega = \mathrm{Re}\left(\frac{\mathrm{i}}{\pi} \ln\left((\mathscr{A} + \omega_2 \mathrm{i}\mathscr{E})(\mathscr{A} + \omega_1 \mathrm{i}\mathscr{E})^{-1} \right) \right) \mathscr{B},$$
$$\mathscr{C}_\Omega = \mathscr{C} \mathrm{Re}\left(\frac{\mathrm{i}}{\pi} \ln\left((\mathscr{A} + \omega_1 \mathrm{i}\mathscr{E})^{-1}(\mathscr{A} + \omega_2 \mathrm{i}\mathscr{E}) \right) \right).$$

Analogously, the time-limited Gramians P_T and Q_T of (10) are given as the unique positive semi-definite solutions of the (potentially) indefinite Lyapunov equations

$$\mathscr{A} P_T \mathscr{E}^\mathsf{T} + \mathscr{E} P_T \mathscr{A}^\mathsf{T} + \mathscr{B}_{t_0} \mathscr{B}_{t_0}^\mathsf{T} - \mathscr{B}_{t_\mathrm{f}} \mathscr{B}_{t_\mathrm{f}}^\mathsf{T} = 0,$$
$$\mathscr{A}^\mathsf{T} Q_T \mathscr{E} + \mathscr{E}^\mathsf{T} Q_T \mathscr{A} + \mathscr{C}_{t_0}^\mathsf{T} \mathscr{C}_{t_0} - \mathscr{C}_{t_\mathrm{f}}^\mathsf{T} \mathscr{C}_{t_\mathrm{f}} = 0,$$

where the time-dependent right-hand sides are defined as

$$\mathscr{B}_{t_0} = \mathrm{e}^{\mathscr{A}\mathscr{E}^{-1}t_0}\mathscr{B}, \quad \mathscr{B}_{t_\mathrm{f}} = \mathrm{e}^{\mathscr{A}\mathscr{E}^{-1}t_\mathrm{f}}\mathscr{B}, \quad \mathscr{C}_{t_0} = \mathscr{C}\mathrm{e}^{\mathscr{E}^{-1}\mathscr{A}t_0}, \quad \mathscr{C}_{t_\mathrm{f}} = \mathscr{C}\mathrm{e}^{\mathscr{E}^{-1}\mathscr{A}t_\mathrm{f}}$$

on the time interval $T = [t_0, t_\mathrm{f}]$. Using those Gramians for the different second-order balanced truncation approaches [7,11,15] leads to the second-order limited balanced truncation methods as described in [31]. The dense version of the resulting methods is contained in the current version of the MORLAB toolbox [32], and an implementation for large-scale sparse systems as MATLAB and GNU Octave toolbox can be found in [33].

As numerical example for the frequency-limited approach, we consider the triple chain oscillator example as in [19]. We reduce the original model ($n = 1\,201$) by the second-order frequency-limited balanced truncation method in the interval $[5 \cdot 10^{-3}, 5 \cdot 10^{-2}]$ rad/sec using the eight different second-order balancing formulas from [31] to the order $r = 34$. The computations are done using the dense implementation of the second-order frequency-limited balanced truncation method from the latest version of the MORLAB toolbox [32]. The results can be seen in Fig. 3 with the transfer functions and the relative approximation errors. The computed reduced-order models are denoted according to the used balancing formulas from [31]. We clearly see the good approximation behavior in the frequency range of interest. Note that only the system computed by the fv formula is stable, while all others become unstable.
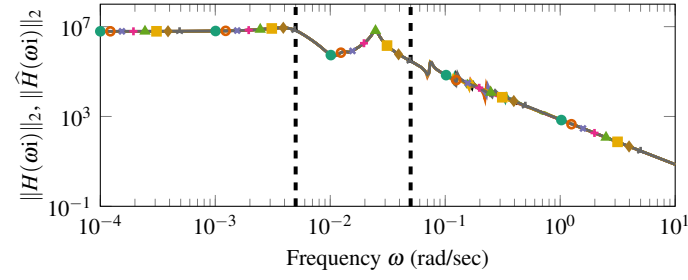
(a) Sigma plots.
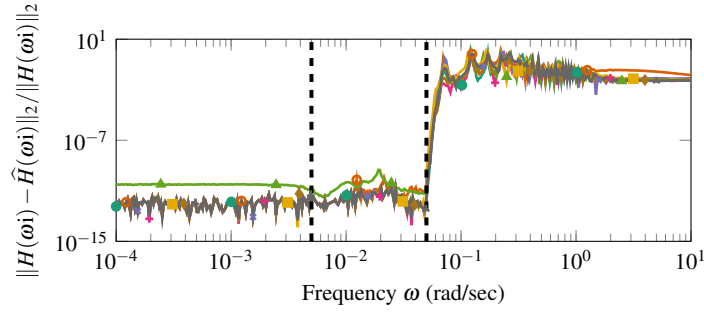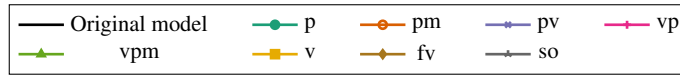

(b) Relative errors.

Fig. 3: Frequency-limited balanced truncation results for the triple chain oscillator example.

To illustrate the time-limited balanced truncation method, we use the single chain oscillator example as described in [31]. Here, we use the implementation for large-scale sparse mechanical systems from [26] to reduce the original system ($n = 12\,000$) to order $r = 3$ in the time interval $[0, 20]$ sec. The results for the second output entry can be seen in Fig. 4, where in the time region of interest, the original system is nicely approximated by the reduced-order models. For all balancing formulas, the resulting systems are stable.

4 Positive real balanced truncation for second-order systems

In this section, we consider second-order systems of the form (1), where $M, K > 0$, $D \geq 0$, and either we exclusively measure positions, i.e., $C_v = 0$, or velocities, i.e., $C_p = 0$. We start with the second case and additionally assume co-located inputs and outputs, which means $B_u = C_v^\mathsf{T}$. This case is treated in [34]. Using the Cholesky
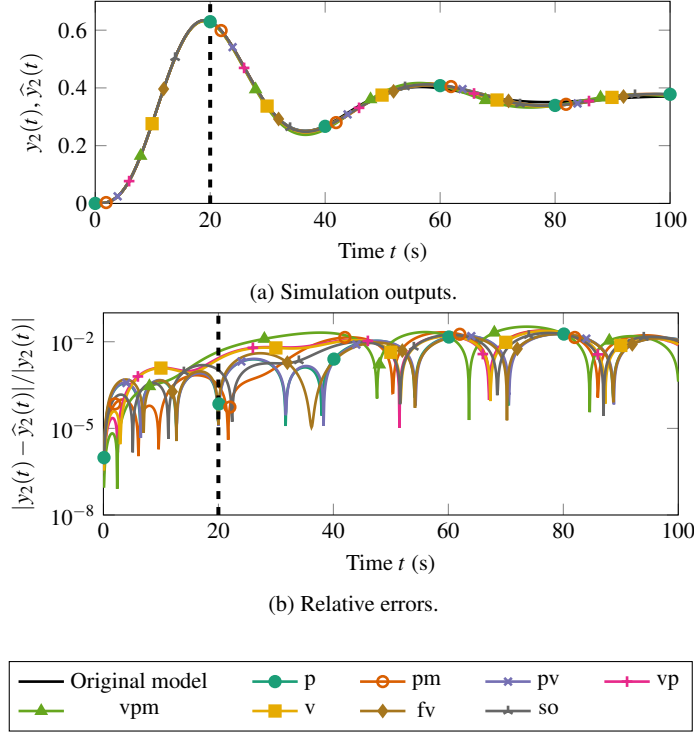
(a) Simulation outputs.

(b) Relative errors.

Fig. 4: Time-limited balanced truncation results for the single chain oscillator example.

factorizations $K = GG^{\mathsf{T}}$ and $M = LL^{\mathsf{T}}$, the system can be rewritten in first-order form as

$$
\dot{x}(t) = \underbrace{\begin{bmatrix} 0 & G^{\mathsf{T}}L^{-\mathsf{T}} \\ -L^{-1}G & -L^{-1}DL^{-\mathsf{T}} \end{bmatrix}}_{=:\mathscr{A}} x(t) + \underbrace{\begin{bmatrix} 0 \\ L^{-1}B_{\mathrm{u}} \end{bmatrix}}_{=:\mathscr{B}} u(t),
$$
$$
y(t) = \underbrace{\begin{bmatrix} 0 & B_{\mathrm{u}}^{\mathsf{T}}L^{-\mathsf{T}} \end{bmatrix}}_{=:\mathscr{C}} x(t).
\tag{11}
$$

Besides passivity, the most important feature of this system is that it has an internal symmetry structure $\mathscr{A}\mathscr{S}_n = \mathscr{S}_n\mathscr{A}^{\mathsf{T}}$ and $\mathscr{C} = \mathscr{B}^{\mathsf{T}} = \mathscr{B}^{\mathsf{T}}\mathscr{S}_n$, where $\mathscr{S}_n :=$ diag$(-I_n, I_n)$. In particular, its transfer function $H(s) = \mathscr{C}(sI_{2n} - \mathscr{A})^{-1}\mathscr{B}$ is symmetric, i.e., it fulfills $H(s)^{\mathsf{T}} = H(s)$. We will make heavy use of this symmetry structure.

The model reduction technique is consisting of two steps:

Step 1: We apply positive real balanced truncation [35] to the first order system (11), whose numerical bottleneck is consisting of the numerical solution of the Lur'e equations

$$\mathscr{A}^\mathsf{T} P + P\mathscr{A} = -K_\mathrm{c}^\mathsf{T} K_\mathrm{c}, \qquad \mathscr{A}Q + Q\mathscr{A}^\mathsf{T} = -K_\mathrm{o}^\mathsf{T} K_\mathrm{o},$$
$$P\mathscr{B} - \mathscr{C}^\mathsf{T} = 0, \qquad\qquad Q\mathscr{C}^\mathsf{T} - \mathscr{B} = 0, \tag{12}$$

for stabilizing solutions $P, Q \in \mathbb{R}^{2n \times 2n}$, see [36]. The internal symmetry structure of (11) yields that $Q = \mathscr{S}_n P \mathscr{S}_n$, whence only the Lur'e equation $\mathscr{A}^\mathsf{T} P + P\mathscr{A} = -K_\mathrm{c}^\mathsf{T} K_\mathrm{c}, P\mathscr{B} - \mathscr{C}^\mathsf{T} = 0$ has to be solved for the matrices P and K_c. We can use the method from [37] to obtain a low-rank approximative solution $P \approx L^\mathsf{T} L$. The sign symmetry of the first order system (11) yields that its positive real characteristic values (which are defined to be the square roots of the eigenvalues of PQ) can in a certain sense be allocated to the symmetry structure of the system (11). More precisely, the positive real characteristic values are the absolute values of the eigenvalues of the symmetric matrix $L\mathscr{S}_n L^\mathsf{T}$, and the signs of these eigenvalues are defined to be the signatures of the respective characteristic values. By truncating equally many states corresponding to positive and negative characteristic values, it is shown that the resulting first order model is – without any further computational effort – of the form

$$\dot{\widehat{x}}(t) = \begin{bmatrix} 0 & 0 & 0 & 0 & 0 & \mathscr{A}_{16} \\ 0 & 0 & 0 & 0 & \mathscr{A}_{25} & \mathscr{A}_{26} \\ 0 & 0 & \mathscr{A}_{33} & \mathscr{A}_{34} & 0 & \mathscr{A}_{36} \\ 0 & 0 & -\mathscr{A}_{34}^\mathsf{T} & \mathscr{A}_{44} & 0 & \mathscr{A}_{46} \\ 0 & -\mathscr{A}_{25}^\mathsf{T} & 0 & 0 & 0 & 0 \\ -\mathscr{A}_{16}^\mathsf{T} & -\mathscr{A}_{26}^\mathsf{T} & -\mathscr{A}_{36}^\mathsf{T} & \mathscr{A}_{46}^\mathsf{T} & 0 & \mathscr{A}_{66} \end{bmatrix} \widehat{x}(t) + \begin{bmatrix} 0 \\ 0 \\ 0 \\ 0 \\ 0 \\ \mathscr{B}_6 \end{bmatrix} u(t),$$
$$\widehat{y}(t) = \begin{bmatrix} 0 & 0 & 0 & 0 & 0 & \mathscr{B}_6^\mathsf{T} \end{bmatrix} \widehat{x}(t), \tag{13}$$

where the block sizes from left to right and from top to bottom are m, ℓ, p, p, ℓ, m, with $r = p + m + \ell$. Note that, if $\mathscr{A}_{33}$ is zero, then it would – by merging some of the blocks – be of the form

$$\dot{\widehat{x}}(t) = \begin{bmatrix} 0 & \widehat{G}^\mathsf{T} \\ -\widehat{G} & -\widehat{D} \end{bmatrix} \widehat{x}(t) + \begin{bmatrix} 0 \\ \widehat{B}_\mathrm{u} \end{bmatrix} u(t),$$
$$\widehat{y}(t) = \begin{bmatrix} 0 & \widehat{B}_\mathrm{u}^\mathsf{T} \end{bmatrix} \widehat{x}(t), \tag{14}$$

which would result in a reduced second-order model (2) with $\widehat{M} = I_r$, $\widehat{K} = \widehat{G}\widehat{G}^\mathsf{T}$, $\widehat{C}_\mathrm{p} = 0$, and $\widehat{C}_\mathrm{v} = \widehat{B}_\mathrm{u}^\mathsf{T}$. This is regrettably not the case in general, whence we apply the following step.

Step 2: We apply a state-space transformation to (13) such that the matrix $\mathscr{A}_{33}$ vanishes. More precisely, we first intend to find some invertible $T \in \mathbb{R}^{2p \times 2p}$ that preserves the symmetry structure, i. e., it fulfills $T^\mathsf{T} \mathscr{S}_p T = \mathscr{S}_p$, and

$$T^{-1} \begin{bmatrix} \mathscr{A}_{33} & \mathscr{A}_{34} \\ -\mathscr{A}_{34}^\mathsf{T} & \mathscr{A}_{44} \end{bmatrix} T = \begin{bmatrix} 0 & \widehat{\mathscr{A}}_{34} \\ -\widehat{\mathscr{A}}_{34}^\mathsf{T} & \widehat{\mathscr{A}}_{44} \end{bmatrix}. \tag{15}$$

Then a state-space transformation with $T = \mathrm{diag}(I_{m+\ell}, T, I_{\ell+m})$ leads to a system which is indeed of the form (14) and can then be rewritten as a second-order system.

Such a transformation is based on techniques from indefinite linear algebra [38], and can be computed without any remarkable computational effort. It is shown that such a transformation is possible, if the reduced first-order system (15) has the property that for all $i = 1, \ldots, p$, the ith characteristic value with negative signature is smaller than the ith characteristic value with positive signature. A sufficient criterion on the original system for the existence of such a transformation is that it is *overdamped*, that is $\left(v^\mathsf{T} Dv\right)^2 > 4\left(v^\mathsf{T} Mv\right)\left(v^\mathsf{T} Kv\right)$ for all $v \in \mathbb{R}^n$.

The resulting second-order system in particular fulfills $\widehat{M}, \widehat{K} > 0$, and it is further shown that $\widehat{D} = \widehat{D}^\mathsf{T}$ has at most m negative eigenvalues. If the original system is overdamped, then even $\widehat{D} > 0$. Moreover, the gap metric distance between the transfer functions $H(s)$ of the original and $\widehat{H}(s)$ of the reduced system is shown to be bounded from above by twice the sum of the truncated positive real characteristic values.

Considering a system dilation, we are able to extend the previously presented reduction to second-order systems with velocity measurements $y(t) = C_\mathrm{p} q(t)$, which are not necessarily co-located to the input. This can be done by considering the extended system

$$M\ddot{q}(t) + D\dot{q}(t) + Kq(t) = \begin{bmatrix} B_\mathrm{u} & C_\mathrm{v}^\mathsf{T} \end{bmatrix} \begin{bmatrix} u_1(t) \\ u_2(t) \end{bmatrix},$$

$$\begin{bmatrix} y_1(t) \\ y_2(t) \end{bmatrix} = \begin{bmatrix} B_\mathrm{u}^\mathsf{T} \\ C_\mathrm{v} \end{bmatrix} \dot{q}(t).$$

This system is again positive real and from the algorithm above we thus obtain a reduced-order system for the extended system as

$$\widehat{M}\ddot{\widehat{q}}(t) + \widehat{D}\dot{\widehat{q}}(t) + \widehat{K}\widehat{q}(t) = \begin{bmatrix} \widehat{B}_\mathrm{u} & \widehat{C}_\mathrm{v}^\mathsf{T} \end{bmatrix} \begin{bmatrix} u_1(t) \\ u_2(t) \end{bmatrix},$$

$$\begin{bmatrix} \widehat{y}_1(t) \\ \widehat{y}_2(t) \end{bmatrix} = \begin{bmatrix} \widehat{B}_\mathrm{u}^\mathsf{T} \\ \widehat{C}_\mathrm{v} \end{bmatrix} \dot{\widehat{q}}(t),$$

$$(16)$$

where $\widehat{B}_\mathrm{u} \in \mathbb{R}^{r \times m}$ and $\widehat{C}_\mathrm{v} \in \mathbb{R}^{p \times r}$. From that we obtain a reduced-order system for (1) as

$$\widehat{M}\ddot{\widehat{q}}(t) + \widehat{D}\dot{\widehat{q}}(t) + \widehat{K}\widehat{q}(t) = \widehat{B}_\mathrm{u} u_1(t),$$

$$\widehat{y}_2(t) = \widehat{C}_\mathrm{v}^\mathsf{T} \widehat{q}(t).$$

$$(17)$$

As the transfer function of (17) is a submatrix of the transfer function of the system (16), and the same holds for the original system, the previously derived error bound also holds in this more general case.

We illustrate the performance of the reduction method above with an example of three coupled mass-spring-damper chains; see [39, Ex. 2]. The triple chain consists of three rows that are coupled via a mass m_0, which is connected to the fixed base with a spring with stiffness k_0. Each row contains g masses, $g + 1$ springs and one damper, which is attached to a wall, see Figure 5. One can write the free system as
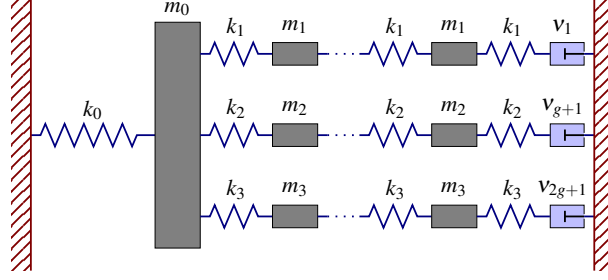
Fig. 5: (3g + 1)-mass (triple chain) oscillator with three dampers [39].

$$M\ddot{q}(t) + D\dot{q}(t) + Kq(t) = 0,$$

where M, D, and K are defined as $M = \mathrm{diag}(m_1, \ldots, m_1, m_2, \ldots, m_2, m_3, \ldots, m_3)$, $D = \alpha M + \beta K + v_1 e_1 e_1^\mathsf{T} + v_{g+1} e_{g+1} e_{g+1}^\mathsf{T} + v_{2g+1} e_{2g+1} e_{2g+1}^\mathsf{T}$ and

$$K = \begin{bmatrix} K_{11} & & & -\kappa_1 \\ & K_{22} & & -\kappa_2 \\ & & K_{33} & -\kappa_3 \\ -\kappa_1^\mathsf{T} & -\kappa_2^\mathsf{T} & -\kappa_3^\mathsf{T} & k_1 + k_2 + k_3 + k_0 \end{bmatrix}, \quad K_{ii} = k_i \begin{bmatrix} 2 & -1 & & & \\ -1 & 2 & -1 & & \\ & \ddots & \ddots & \ddots & \\ & & -1 & 2 & -1 \\ & & & -1 & 2 \end{bmatrix}$$

with $\kappa_i = \begin{bmatrix} 0 \ldots 0 \ k_i \end{bmatrix}^\mathsf{T} \in \mathbb{R}^{1 \times g}$ and $K_{ii} \in \mathbb{R}^{g \times g}$ for $i = 1, 2, 3$. We choose the input $B_\mathrm{u} = \begin{bmatrix} 1 \ldots 1 \end{bmatrix}^\mathsf{T}$ and equally measure the velocities such that $C_\mathrm{v} = B_\mathrm{u}^\mathsf{T}$. The second-order control system reads

$$M\ddot{q}(t) + D\dot{q}(t) + Kq(t) = B_\mathrm{u} u(t),$$
$$y(t) = C_\mathrm{v} \dot{q}(t).$$

We consider the triple chain with $g = 500$, thus the number of differential equations is $n = 3g + 1 = 1\,501$. The stiffness and mass parameters are set as

$$k_0 = 50, \quad k_1 = 10, \quad k_2 = 20, \quad k_3 = 1,$$
$$m_0 = 1, \quad m_1 = 1, \quad m_2 = 2, \quad m_3 = 3$$

and the damping parameters $\alpha = \beta = 0.002$ and $v_1 = v_{g+1} = v_{2g+1} = 5$.

Following the previously presented theory, we first compute a reduced-order model in first-order form of order $2r = 300$ and then recover the structure of a second-order model of order $r = 150$. The latter has again the form

$$\widehat{M}\ddot{\widehat{q}}(t) + \widehat{D}\dot{\widehat{q}}(t) + \widehat{K}\widehat{q}(t) = \widehat{B}_\mathrm{u} u(t), \quad \widehat{y}(t) = \widehat{B}_\mathrm{u}^\mathsf{T} \dot{\widehat{q}}(t),$$

(a) Sigma plots.

(b) Relative error.

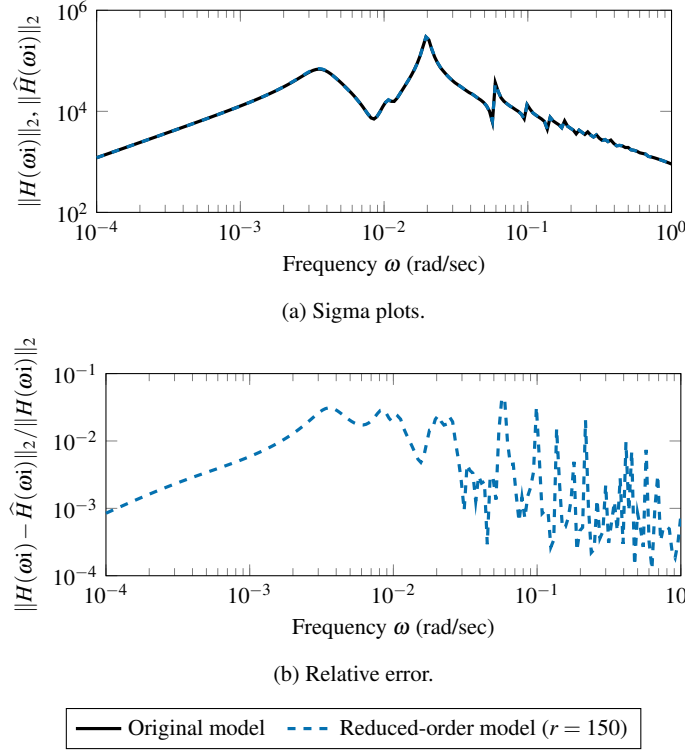| —— Original model | - - - Reduced-order model ($r = 150$) |

Fig. 6: Positive real balanced truncation results for the triple chain oscillator example.

with symmetric $\widehat{M}, \widehat{D}, \widehat{K} \in \mathbb{R}^{r \times r}$ and $\widehat{B}_{\mathrm{u}} \in \mathbb{R}^{r \times m}$, where $\widehat{M} = I_r$, $\widehat{K} > 0$ and $\widehat{D} = \widehat{D}^{\mathsf{T}}$ has one negative eigenvalue $\lambda \approx -3.535 \cdot 10^{-2}$, while its largest eigenvalue is $\lambda_{\max} \approx 3.162$. The plot of the absolute value of the original and reduced transfer function together can be found in Figure 6a, whereas Figure 6b displays the relative error of the transfer function on the imaginary axis, respectively. With a maximum relative error of approximately $4.3 \cdot 10^{-2}$ we obtain a good match between the original and the reduced second-order system.

5 $\mathcal{H}_\infty$-optimal rational approximation

In this section, we briefly describe an interpolatory $\mathcal{H}_\infty$ model order reduction scheme for systems with symmetric mass damping and stiffness matrices and co-located inputs and outputs, i. e., we have $M, D, K > 0$, $B_{\mathrm{u}} = C_{\mathrm{p}}^{\mathsf{T}}$ and $C_{\mathrm{v}} = 0$ in order to be able to preserve symmetry and asymptotic stability by an appropriate choice of the projection spaces. More precisely, we construct a sequence of reduced-order

transfer functions of the form

$$\widehat{H}_j(s) := B_{\mathrm{u}}^{\mathsf{T}} V_j \big(s^2 V_j^{\mathsf{T}} M V_j + s V_j^{\mathsf{T}} D V_j + V_j^{\mathsf{T}} K V_j \big)^{-1} V_j^{\mathsf{T}} B_{\mathrm{u}}, \quad j = 1, 2, \dots$$

for appropriately chosen truncation matrices V_j. Our method aims to iteratively reduce the $\mathscr{H}_\infty$-norm of the error transfer function $\mathscr{E}_j(s) := H(s) - \widehat{H}_j(s)$. To do so, we evaluate $\big\|\mathscr{E}_j\big\|_{\mathscr{H}_\infty} := \max_{\omega \in \mathbb{R} \cup \{\infty\}} \big\|E_j(\omega \mathrm{i})\big\|_2 = \big\|\mathscr{E}_j(\omega \mathrm{i})\big\|_2$ and choose $V_{j+1} := \big[V_j \ (-\omega_j^2 M + \omega_j \mathrm{i} D + K)^{-1} B_{\mathrm{u}}\big]$. This choice guarantees Hermite interpolation properties between the original and reduced transfer functions $H(s)$ and $\widehat{H}_j(s)$ at the interpolation points $\omega_1 \mathrm{i}, \omega_2 \mathrm{i}, \dots, \omega_j \mathrm{i}$, such that the error near these points becomes small. This procedure is repeated until a specified error tolerance is met.

The main computational cost of this algorithm is the repeated computation of the $\mathscr{H}_\infty$-norm of the error transfer function, which is expensive to evaluate since the error system is of large dimension. However, these computations have been made possible by the methods presented in [40, 41], which we use here and which work as follows.

Assume that a transfer function is given by $H(s) = C(sE - A)^{-1}B$ with the regular matrix pencil $sE - A \in \mathbb{R}[s]^{n \times n}$, $B \in \mathbb{R}^{n \times m}$, and $C \in \mathbb{R}^{p \times n}$ with $n \gg m, p$. Then the algorithm determines a sequence of reduced-order transfer functions of the form $H_j(s) = C V_j (s W_j^{\mathsf{H}} E V_j - W_j^{\mathsf{H}} A V_j)^{-1} W_j^{\mathsf{H}} B$, where $V_j, W_j \in \mathbb{C}^{n \times k_j}$ and $k_j \ll n$ for $j = 1, 2, \dots$, and where $\big\|H_j\big\|_{\mathscr{L}_\infty} := \max_{\omega \in \mathbb{R} \cup \{\infty\}} \big\|H_j(\omega \mathrm{i})\big\|_2$ converges to $\|H\|_{\mathscr{H}_\infty}$. Since the matrices defining the reduced-order transfer functions $H_j(s)$, are of small dimensions, $\big\|H_j\big\|_{\mathscr{L}_\infty}$ can be efficiently computed using well-established methods such as [42, 43]. Assume first that $m = p$. Further suppose that j interpolation points $\omega_1 \mathrm{i}, \dots, \omega_j \mathrm{i} \in \mathrm{i}\mathbb{R}$ are already given. In this case, the truncation matrices are chosen as

$$V_j = \big[(\omega_1 \mathrm{i} E - A)^{-1} B \ \dots \ (\omega_j \mathrm{i} E - A)^{-1} B\big],$$
$$W_j = \big[(\omega_1 \mathrm{i} E - A)^{-\mathsf{H}} C^{\mathsf{H}} \ \dots \ (\omega_j \mathrm{i} E - A)^{-\mathsf{H}} C^{\mathsf{H}}\big].$$

This choice of the truncation matrices amounts to the Hermite interpolation conditions

$$H(\omega_k \mathrm{i}) = H_j(\omega_k \mathrm{i}), \quad H'(\omega_k \mathrm{i}) = H_j'(\omega_k \mathrm{i}), \quad k = 1, \dots, j,$$

that carry over directly to the functions $\sigma(s) := \|H(s)\|_2$ and $\sigma_j(s) := \big\|H_j(s)\big\|_2$. These Hermite interpolation conditions are then used to prove a superlinear rate of convergence to a local maximum of $\sigma(\mathrm{i}\cdot)$ provided that the algorithm converges. The situation is more difficult if $m \neq p$ since then, V_j and W_j would have different dimensions and the pencil $s W_j^{\mathsf{H}} E V_j - W_j^{\mathsf{H}} A V_j$ would be singular. This situation also occurs, if V_j or W_j do not have full column rank. Thus, an alternative choice for V_j and W_j, which is outlined in [40], and QR factorizations can be used to obtain the truncation matrices such that the pencil $s W_j^{\mathsf{H}} E V_j - W_j^{\mathsf{H}} A V_j$ is regular.

In Figure 7, we illustrate the effectiveness of our algorithm using the triple chain oscillator benchmark example [39] of order $n = 1\,000$ and an $\mathscr{H}_\infty$-error bound of
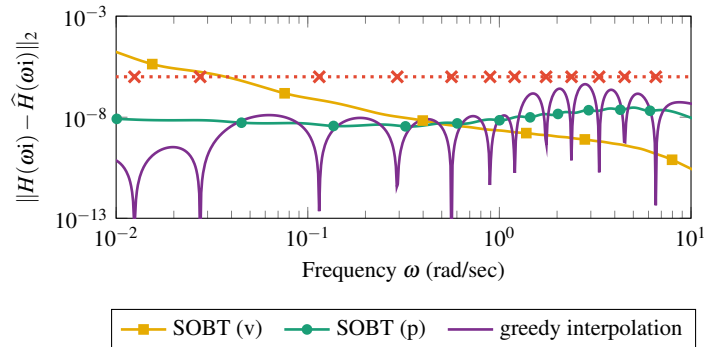
Fig. 7: Comparison of absolute errors of different methods for second-order model reduction. The interpolation points of our greedy approach are plotted as red crosses.

10^{-6}. Compared with two different second-order balanced truncation (SOBT) approaches from [15], the greedy interpolation approach has a slightly larger maximal error for the same reduced order $r = 29$. However, in contrast to SOBT, we obtain full information on the current error and may terminate whenever the reduced-order model satisfies a prescribed error bound. Moreover, the method also allows for an easy adaptation to frequency-limited reduction. We currently investigate post-processing strategies to improve the performance of the greedy interpolation such as an additional optimization of the interpolation points. Furthermore, our approach may be combined with the subspaces obtained from (SO)BT to initialize the first projection space.

The previously described algorithm leads to an error function $\mathscr{E}_j(s)$, which is zero at the interpolation points in exact arithmetics. This results in the spiky shape of the error maximum singular value function that can be observed in Fig. 7. Such a behavior is generally unwanted, since this indicates that our ROM approximates the given model at a few frequencies much better than at others. In this way, accuracy is "wasted" in a few regions that could be used to improve the overall accuracy of the ROM. This is an inherent problem of a greedy approximation strategy with interpolation on the imaginary axis.

To smoothen the error maximum singular value function and reach a better approximation with respect to the $\mathscr{H}_\infty$-norm, we use direct numerical optimization. In particular, after a new interpolation point has been chosen according to the previously described greedy algorithm, we vary the interpolation points such that the $\mathscr{H}_\infty$-error is locally minimized. This requires the solution of a nonsmooth, nonconvex and nonlinear optimization problem. We use the method described in [44] implemented in the software package GRANSO[1]. This iterative optimization requires the repeated evaluation of the $\mathscr{H}_\infty$-norm of the error system, which is high-dimensional. For that, we again apply the method described in [40], which is well-suited for this task.

---

[1] available at http://www.timmitchell.com/software/GRANSO

It is important to note that the gradient of $\|\mathscr{E}_j\|_{\mathscr{H}_\infty}$ with respect to the interpolation points can be computed analytically. Furthermore, the direct optimization strategy is not limited to just the interpolation points. On top of that, we can optimize *tangential directions* of the interpolation as well. In case of tangential interpolation, the truncation matrix can be chosen as

$$V_j = \left[(s_1^2 M + s_1 D + K)^{-1} B_\mathrm{u} b_1 \ \ldots \ (s_j^2 M + s_j D + K)^{-1} B_\mathrm{u} b_j \right],$$

where $b_k \in \mathbb{C}^m$, and $s_k \in \mathbb{C}$ for $k = 1, \ldots, j$ not being in the spectrum of $s^2 M + s D + K$. In this way, the interpolation condition is relaxed such that we now only have *tangential* Hermite interpolation between $H(s)$ and $\widehat{H}_j(s)$, that is

$$H(s_k)b_k = \widehat{H}_j(s_k)b_k, \quad b_k^\mathsf{H} H(s_k) = b_k^\mathsf{H} \widehat{H}_j(s_k), \quad b_k^\mathsf{H} H'(s_k)b_k = b_k^\mathsf{H} \widehat{H}_j'(s_k)b_k,$$

for $k = 1, \ldots, j$. This results in an optimization that can exploit more degrees of freedom, while the size of the projection matrix and hence the size of the ROM is further reduced.
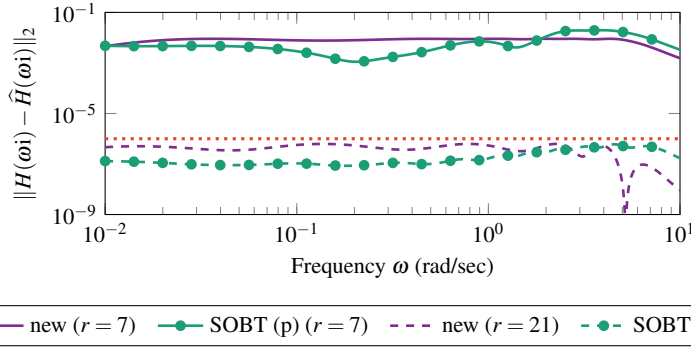
Fig. 8: Comparison of the (absolute) errors of SOBT (p) with the new, optimization-based method.

In Figure 8, we show a comparison of the errors between this new method and (the faster) SOBT on the triple chain oscillator example with $n = 301$. The new method leads to an error function that is more steady and even outperforms the SOBT methods for the smaller reduced model order. However, for the slightly larger model order that is required to meet the given error bound of 10^{-6}, the optimization got stuck in a local optimum. Therefore, the error is less steady. However, the accuracy is still comparable with the accuracy obtained by SOBT.

6 Conclusions

We have presented an overview of recently developed structure-preserving model order reduction methods for second-order systems. We have started with an adaptation of the dominant pole algorithm for modally damped mechanical systems and, afterwards, have introduced extensions of the frequency- and time-limited balanced truncation methods for second-order systems in various ways. We have presented an approach for structure recovery of second-order systems based on positive real balanced truncation, which also yields an a priori error bound in the gap metric, and concluded with an $\mathscr{H}_\infty$ greedy interpolation approach yielding an $\mathscr{H}_\infty$-error optimal approximation. Numerical examples for all the presented approaches have illustrated their effectiveness.

Additionally to the approaches for linear systems summarized here, we were able to develop model order reduction techniques for (parametric) mechanical systems with special nonlinearities, namely bilinear control systems and quadratic-bilinear systems. These techniques will be subject to further research and be described in a different work.

References

1. A.C. Antoulas, *Approximation of Large-Scale Dynamical Systems*, *Adv. Des. Control*, vol. 6 (SIAM Publishing, Philadelphia, PA, 2005). doi:10.1137/1.9780898718713
2. P. Benner, V. Mehrmann, D.C. Sorensen, *Dimension Reduction of Large-Scale Systems*, *Lect. Notes Comput. Sci. Eng.*, vol. 45 (Springer-Verlag, Berlin/Heidelberg, Germany, 2005). doi:10.1007/3-540-27909-1
3. A. Quarteroni, G. Rozza, *Reduced Order Methods for Modeling and Computational Reduction*, *MS&A – Modeling, Simulation and Applications*, vol. 9 (Springer International Publishing, Cham, Switzerland, 2014). doi:10.1007/978-3-319-02090-7
4. P. Benner, A. Cohen, M. Ohlberger, K. Willcox (eds.), *Model Reduction and Approximation: Theory and Algorithms*. Computational Science & Engineering (SIAM Publications, Philadelphia, PA, 2017). doi:10.1137/1.9781611974829
5. P. Benner, W. Schilders, S. Grivet-Talocia, A. Quarteroni, G. Rozza, L.M. Silveira, *Model Order Reduction* (De Gruyter, Berlin, Boston, 2021). URL https://www.degruyter.com/view/title/523453
6. T.T. Georgiou, M.C. Smith, IEEE Trans. Automat. Control **35**(6), 673 (1990). doi:10.1109/9.53546
7. D.G. Meyer, S. Srinivasan, IEEE Trans. Automat. Control **41**(11), 1632 (1996). doi:10.1109/9.544000
8. Z. Bai, Y.F. Su, SIAM J. Sci. Comput. **26**(5), 1692 (2005)
9. R.W. Freund, in *Dimension Reduction of Large-Scale Systems*, *Lect. Notes Comput. Sci. Eng.*, vol. 45, ed. by P. Benner, V. Mehrmann, D.C. Sorensen (Springer-Verlag, Berlin/Heidelberg,

Germany, 2005), *Lect. Notes Comput. Sci. Eng.*, vol. 45, pp. 173–189. doi:10.1007/3-540-27909-1_8

10. B. Salimbahrami, B. Lohmann, Linear Algebra Appl. **415**(2–3), 385 (2006). doi:10.1016/j.laa.2004.12.013

11. Y. Chahlaoui, D. Lemonnier, A. Vandendorpe, P. Van Dooren, Linear Algebra Appl. **415**(2–3), 373 (2006). doi:10.1016/j.laa.2004.03.032

12. C. Hartmann, V.M. Vulcanov, C. Schütte, Multiscale Model. Simul. **8**(4), 1348 (2010). doi:10.1137/080732717

13. P. Benner, J. Saak, Math. Comput. Model. Dyn. Syst. **17**(2), 123 (2011). doi:10.1080/13873954.2010.540822

14. P. Benner, P. Kürschner, J. Saak, Math. Comput. Model. Dyn. Syst. **19**(6), 593 (2013). doi:10.1080/13873954.2013.794363

15. T. Reis, T. Stykel, Math. Comput. Model. Dyn. Syst. **14**(5), 391 (2008). doi:10.1080/13873950701844170

16. B. Salimbahrami, Structure preserving order reduction of large scale second order models. Dissertation, Technische Universität München, Munich, Germany (2005). URL https://mediatum.ub.tum.de/doc/601950/00000941.pdf

17. C.A. Beattie, S. Gugercin, Systems Control Lett. **58**(3), 225 (2009). doi:10.1016/j.sysconle.2008.10.016

18. H.K.F. Panzer, T. Wolf, B. Lohmann, in *2013 European Control Conference (ECC), July 17-19, 2013, Zürich, Switzerland* (2013), pp. 4484–4489. doi:10.23919/ECC.2013.6669657

19. R.S. Beddig, P. Benner, I. Dorschky, T. Reis, P. Schwerdtner, M. Voigt, S.W.R. Werner, Proc. Appl. Math. Mech. **19**(1), e201900224 (2019). doi:10.1002/pamm.201900224

20. E.J. Davison, IEEE Trans. Automat. Control **AC–11**, 93 (1966). doi:10.1109/TAC.1966.1098264

21. N. Martins, L.T.G. Lima, H.J.C.P. Pinto, IEEE Trans. Power Syst. **11**(1), 162 (1996). doi:10.1109/59.486093

22. J. Rommes, N. Martins, IEEE Trans. Power Syst. **21**(4), 1471 (2006). doi:10.1109/TPWRS.2006.881154

23. P. Benner, P. Kürschner, Z. Tomljanović, N. Truhar, ZAMM Z. Angew. Math. Mech. **96**(5), 604 (2016). doi:10.1002/zamm.201400158

24. C.A. Beattie, P. Benner, $\mathscr{H}_2$-optimality conditions for structured dynamical systems. Preprint MPIMD/14-18, Max Planck Institute Magdeburg (2014). URL https://www2.mpi-magdeburg.mpg.de/preprints/2014/18/

25. J. Saak, D. Siebelts, S.W.R. Werner, at-Automatisierungstechnik **67**(8), 648 (2019). doi:10.1515/auto-2019-0027

26. P. Benner, S.W.R. Werner. SOMDDPA – Second-Order Modally-Damped Dominant Pole Algorithm (version 1.1) (2020). doi:10.5281/zenodo.3332706

27. Oberwolfach Benchmark Collection. Butterfly gyroscope. hosted at MORwiki – Model Order Reduction Wiki (2004). URL http://modelreduction.org/index.php/Butterfly_Gyroscope

28. W. Gawronski, J.N. Juang, Int. J. Syst. Sci. **21**(2), 349 (1990). doi:10.1080/00207729008910366

29. K. Haider, A. Ghafoor, M. Imran, F.M. Malik, Asian J. Control **20**(2), 790 (2018). doi:10.1002/asjc.1598

30. K. Haider, A. Ghafoor, M. Imran, F.M. Malik, Trans. Inst. Meas. Control **41**(8), 2310 (2019). doi:10.1177/0142331218798893

31. P. Benner, S.W.R. Werner, Linear Algebra Appl. (2020). doi:10.1016/j.laa.2020.06.024. Article in press

32. P. Benner, S.W.R. Werner. MORLAB – Model Order Reduction LABoratory (version 5.0) (2019). doi:10.5281/zenodo.3332716. See also: http://www.mpi-magdeburg.mpg.de/projects/morlab

33. P. Benner, S.W.R. Werner. Limited balanced truncation for large-scale sparse second-order systems (version 2.0) (2020). doi:10.5281/zenodo.3331592

34. I. Dorschky, T. Reis, M. Voigt, Balanced truncation model reduction for symmetric second order systems – A passivity-based approach. e-print 2006.09170, arXiv (2020). URL https://arxiv.org/abs/2006.09170

35. C. Guiver, M.R. Opmeer, Linear Algebra Appl. **439**(12), 3659 (2013). doi:10.1016/j.laa.2013.09.032

36. T. Reis, Linear Algebra Appl. **434**(1), 152 (2011). doi:10.1016/j.laa.2010.09.005

37. F. Poloni, T. Reis, SIAM J. Matrix Anal. Appl. **33**(4), 1339 (2012). doi:10.1137/120861679

38. I. Gohberg, P. Lancaster, L. Rodman, *Matrices and Indefinite Scalar Products* (Birkhäuser, Basel, 1983)

39. N. Truhar, K. Veselić, SIAM J. Matrix Anal. Appl. **31**(1), 18 (2009). doi:10.1137/070683052

40. N. Aliyev, P. Benner, E. Mengi, P. Schwerdtner, M. Voigt, SIAM J. Matrix Anal. Appl. **38**(4), 1496 (2017). doi:10.1137/16M1086200

41. P. Schwerdtner, M. Voigt, IFAC-PapersOnLine **51**(25), 84 (2018). doi:10.1016/j.ifacol.2018.11.086. 9th IFAC Symposium on Robust Control Design ROCOND 2018, Florianópolis, Brazil

42. S. Boyd, V. Balakrishnan, Systems Control Lett. **15**(1), 1 (1990). doi:10.1016/0167-6911(90)90037-U

43. P. Benner, V. Sima, M. Voigt, IEEE Trans. Automat. Control **57**(1), 233 (2012). doi:10.1109/TAC.2011.2161833

44. F.E. Curtis, T. Mitchell, M.L. Overton, Optim. Methods Softw. **32**(1), 148 (2017). doi:10.1080/10556788.2016.1208749